International Journal of Science and Research (IJSR)
ISSN (Online): 2319-7064
Index Copernicus Value (2013): 6.14 | Impact Factor (2013): 4.438

An Enhanced Microgrid Load Sharing by using PI & Fuzzy Controllers

Sk. Abdul Shaheel[1], Sk. Hameed[2]

[1]M.Tech Student Scholar, Department of Electrical and Electronics Engineering
Quba College of Engineering and Technology, Affiliated to JNTUA, Anatapur, SPSR Nellore (dt); A.P, India

[2]M. Tech.,HOD & Sr. Professor, Department of Electrical and Electronics Engineering
Quba College of Engineering and Technology, Affiliated to JNTUA, Anatapur, SPSR Nellore (dt); A.P, India

Abstract: ***The main task of autonomous microgrids is to share the load demand using multiple distributed generation (DG) units. In order to realize satisfied power sharing without the communication between DG units. This paper proposes a fuzzy based enhanced control strategy to estimate the reactive power control error through injecting small real power disturbances for improving the accuracy. An accurate reactive power sharing achieves in the proposed compensation method at the steady state. Simulation results are carried out by MATLAB Software.***

Keywords: Distributed generation (DG), droop control, micro-grid, reactive power compensation, real and reactive power sharing, fuzzy logic controller.

1. Introduction

The application of distributed power generation has been increasing rapidly in the past decades. Compared to the conventional centralized power generation, distributed generation (DG) units deliver clean and renewable power close to the customer's end. Therefore, it can alleviate the stress of many conventional transmission and distribution infrastructures. As most of the DG units are interfaced to the grid using power electronics Converters, they have the opportunity to realize enhanced Power generation through a flexible digital control of the power converters.

On the other hand, high penetration of power electronics based DG units also introduces a few issues, such as system Resonance, protection interference, etc. In order to overcome these problems, the microgrid concept has been proposed, which is realized through the control of multiple DG units.

Compared to a single DG unit, the microgrid can achieve superior power management within its distribution networks. In addition, the islanding operation of microgrid offers high reliability power supply to the critical loads. Therefore, microgrid is considered to pave the way to the future smart grid.

In an islanded microgrid, the loads must be properly shared by multiple DG units. Conventionally, the frequency and voltage magnitude droop control is adopted, which aims to achieve microgrid power sharing in a decentralized manner. However, the droop control governed microgrid is prone to have some power control stability problems when the DG feeders are mainly resistive. It can also be seen that the real power sharing at the steady state is always accurate while the reactive power sharing is sensitive to the impacts of mismatched feeder impedance. Moreover, the existence of local loads and the networked microgrid configurations often further aggravate reactive power sharing problems.

To solve the power control issues, a few improved methods have been proposed. In, the virtual frequency–voltage frame and virtual real and reactive power concept were developed, which improve the stability of the microgrid system. However, these methods cannot suppress the reactive power sharing errors at the same time. Additionally, when small synchronous generators are incorporated into the microgrid, proper power sharing between inverter-based DG units and electric machine based DG units will be more challenging in these methods.

In, both the reactive power and the harmonic power sharing errors were reduced with the non-characteristic harmonic current injection. Although the power sharing problem was addressed, the corresponding steady-state voltage distortions degrade the microgrid power quality. In, a "Q–V dot droop" method was presented. It can be observed from that the reactive power sharing improvement is not obvious when local loads are included.

A. Distributed Generation

Distributed generation, also called on-site generation, dispersed generation, embedded generation, decentralized generation, decentralized energy or distributed energy generates electricity from many small energy sources. Currently, industrial countries generate most of their electricity in large centralized facilities, such as fossil fuel (coal, gas powered) nuclear or hydropower plants. These plants have excellent economies of scale, but usually transmit electricity long distances and negatively affect the environment. Most plants are built this way due to a number of economic, health & safety, logistical, environmental, and geological factors. For example, coal power plants are built away from cities to prevent their heavy air pollution from affecting the populace. In addition, such plants are often built near collieries to minimize the cost of transporting coal. Hydroelectric plants are by their nature limited to operating at sites with sufficient water flow. Most power plants are often considered to be too far away for their waste heat to be used for heating buildings.

Low pollution is a crucial advantage of combined cycle plants that burn natural gas. The low pollution permits the plants to be near enough to a city to be used for district heating and cooling. Distributed generation is another approach. It reduces the amount of energy lost in transmitting electricity because the electricity is generated very near where it is used, perhaps even in the same building. This also reduces the size and number of power lines that must be constructed. Typical distributed power sources in a Feed-in Tariff (FIT) scheme have low maintenance, low pollution and high efficiencies. In the past, these traits required dedicated operating engineers and large complex plants to reduce pollution. However, modern embedded systems can provide these traits with automated operation and renewable, such as sunlight, wind and geothermal. This reduces the size of power plant that can show a profit.

B. Distributed Energy Resource

Distributed energy resource (DER) systems are small-scale power generation technologies (typically in the range of 3 kW to 10,000 kW) used to provide an alternative to or an enhancement of the traditional electric power system. The usual problems with distributed generators are their high costs.

One popular source is solar panels on the roofs of buildings. Some solar cells ("thin-film" type) also have waste disposal issues, since "thin-film" type solar cells often contain heavy-metal electronic wastes, such as Cadmium telluride (CdTe) and Copper indium gallium selenide (CuInGaSe), and need to be recycled. As opposed to silicon semi-conductor type solar cells which is made from quartz. The plus side is that unlike coal and nuclear, there are no fuel costs, pollution, mining safety or operating safety issues. Solar also has a low duty cycle, producing peak power at local noon each day. Average duty cycle is typically 20%.

Another source is small wind turbines. These have low maintenance, and low pollution. Construction costs are higher than large power plants, except in very windy areas. Wind towers and generators have substantial insurable liabilities caused by high winds, but good operating safety. In some areas of the US there may also be property tax costs involved with wind turbines that are not offset by incentives or accelerated depreciation. Wind also tends to be complementary to solar; on days there is no sun there tends to be wind and vice versa. Many distributed generation sites combine wind power and solar power.

2. Modeling of Case Study Analysis of the Conventional Droop Control Method

A. Operation of Microgrid

Fig. 1. illustrates the configuration of a microgrid. As shown, the microgrid is composed of a number of DG units and loads. Each DG unit is interfaced to the microgrid with an inverter, and the inverters are connected to the common AC bus through their respective feeders. Considering that the focus of this paper is the fundamental real and reactive power control, nonlinear loads are not considered in the microgrid. The microgrid and main grid status are monitored by the secondary central controller. According to the operation requirements, the microgrid can be connected (grid-connected mode) or disconnected (islanding mode) from the main grid by controlling the static transfer switch (STS) at the point of common coupling (PCC).

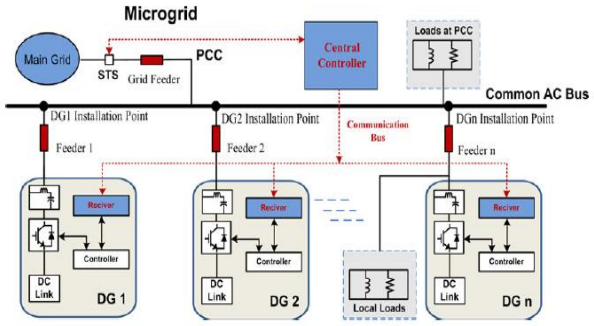

Figure 1: Illustration of the microgrid configuration [1].

During the grid-connected operation, real and reactive power references are normally assigned by the central controller and the conventional droop control method can be used for power tracking. However, to eliminate the steady-state reactive power tracking errors, the PI regulation for the voltage magnitude control was developed. Therefore, power sharing is not a real concern during the grid-connected operation [1]. When the microgrid is switched to islanding operation, the total load demand of the microgrid must be properly shared by these DG units.

During the islanding operation, DG units as illustrated in Fig. 1, can operate using the conventional real power–frequency droop control and reactive power–voltage magnitude droop control as

$$\omega = \omega_0 - D_P \cdot P \quad (1)$$

$$E = E_0 - D_Q \cdot Q \quad (2)$$

Where ω_0 and E_0 are the nominal values of DG angular frequency and DG voltage magnitude respectively, P and Q are the measured real and reactive powers after the first-order low-pass filtering (LPF), D_P and D_Q are the real and reactive power droop slopes. With the derived angular frequency and voltage magnitude in (1) and (2), the instantaneous voltage reference can be obtained accordingly [1].

B. Reactive Power Sharing Analysis

It is not straightforward to evaluate the reactive power sharing accuracy in a complex networked microgrid. For the sake of simplicity, this section first considers a simplified microgrid with two DG units at the same power rating. The configuration is shown in Fig. 2(a), where each DG unit has a local load. R_1 and X_1, and R_2 and X_2 are the feeder impedances of DG1 and DG2, respectively.

Further considering that DG units are often equipped with series virtual inductors to ensure the stability of the system, the corresponding equivalent circuit is sketched in Fig. 2(b). As shown in Fig. 2(b), the virtual reactances X_{V1} and X_{V2} are placed at the outputs of voltage sources. The magnitudes of the voltage sources are obtained in (3) and (4) as

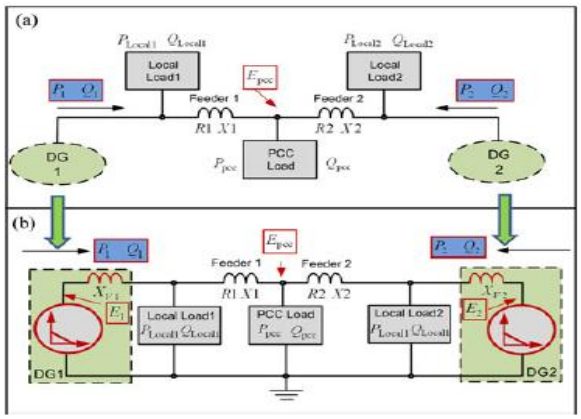

Figure 2: Power flow in a simple microgrid: (a) configuration of the microgrid; (b) equivalent circuit model considering a virtual impedance control [1].

$$E_1 = E_0 - D_Q . Q_1 \quad (3)$$

$$E_2 = E_0 - D_Q . Q_2 \quad (4)$$

Where E_1 and E_2 are the DG voltage magnitudes regulated by the droop control, and Q_1 and Q_2 are the output reactive powers of DG1 and DG2, respectively.

For the power flowing through either physical or virtual impedance, its associated voltage drop on the impedance yields the following approximation as

$$\Delta V \approx \frac{X.Q+R.P}{Eo} \quad (5)$$

Where P and Q are the real and reactive powers at the power sending end of the impedance, R and X are the corresponding resistive and inductive components of the impedance, E_0 is the nominal voltage magnitude, and ΔV is the voltage magnitude drop on the impedance.

Applying the voltage drop approximation (5) to the presented system in Fig. 2(b), the relationships between DG voltages (E_1 and E_2) and the PCC voltage (E_{PCC}) can be established in (6) and (7) as

$$E_1 = E_{PCC} + \frac{X_1(Q_1 - Q_{local1}) + R_1(P_1 - P_{local1})}{E_0} + \frac{X_{v1}.Q_1}{E_0} \quad (6)$$

$$E_2 = E_{PCC} + \frac{X_2(Q_2 - Q_{local2}) + R_2(P_2 - P_{local2})}{E_0} + \frac{X_{v2}.Q_2}{E_0} \quad (7)$$

It is important to note that with system frequency as the communication link, the real power sharing using the conventional droop control is always accurate. Therefore, for the illustrated system at the steady state, the output real powers of DG1 and DG2 are obtained as

$$P_1 = P_2 = 0.5\, P_{Total} = 0.5\, (P_{pcc} + P_{Local1} + P_{Local2} + P_{Feeder1} + P_{Feeder2}) \quad (8)$$

Where P_{Total} means the real power demand within the islanded microgrid, and $P_{Feeder1}$ and $P_{Feeder2}$ are the real power loss on the feeders. Similarly, the reactive power demand (Q_{Total}) is defined as

$$Q_{Total} = Q_{pcc} + Q_{Local1} + Q_{Local2} + Q_{Feeder1} + Q_{Feeder2} \quad (9)$$

Where, $Q_{Feeder1}$ and $Q_{Feeder2}$ are the reactive power loss on the feeders.

By solving the obtained formulas from (3) to (7), the reactive power sharing error ($Q_1 - Q_2$) can be derived. It can be noticed that the reactive power sharing error is related to a few factors, which include the offsets of local loads, unequal voltage drops on virtual and physical impedances, and the variations of the droop slope D_Q.

When all these factors considered at the same time, the evaluation of DG reactive sharing errors is not very straight forward even only two identical DG units are included in the analysis. Due to the complexity of the circuit model, the impacts of different factors shall be studied separately. For instance, the impacts of unequal feeder reactance to reactive power sharing error can be studied by ignoring the effects of local loads, feeder resistance, and virtual impedance. Where the ideal inductive feeder leads to a linear relationship between the DG output reactive power and the magnitude difference between PCC voltage (E_{pcc}) and DG voltages (E_1 and E_2). The relationships are named as "DG1 feeder characteristics" and "DG2 feeder characteristics". With the mismatched feeder reactance ($X_1 < X_2$), the output reactive power of DG unit1 (Q_1) is higher than that of DG unit2 (Q_2) even when same droop slope (D_Q) is adopted for both DG units. It can also be observed that deeper droop slope D^*_Q might alleviate the reactive power sharing errors ($Q^*_1 - Q^*_2$). However, the nontrivial feeder impedance may affect this error as well.

3. Proposed Reactive Power Sharing Error Compensation Method

This section is to develop an enhanced compensation method that can eliminate the reactive power sharing errors without knowing the detailed microgrid configuration. This feature is very important to achieve the "plug-and-play" operation of DG units and loads in the microgrid. To initialize the compensation, the proposed method adopts a low-bandwidth communication link to connect the secondary central controller with DG local controllers [10]. The commutation link sends out the synchronized compensation flag signals from the central controller to each DG unit, so that all the DG units can start the compensation at the same time.

In the proposed compensation method, only one-way communication from the central controller to DG local controllers is needed for starting the DG compensation in a synchronized manner. The intercommunication among DG units is not necessary, so that the plug-and-play feature of a DG unit will not be affected. The simulink diagram of the test system is illustrated in Fig. 3.

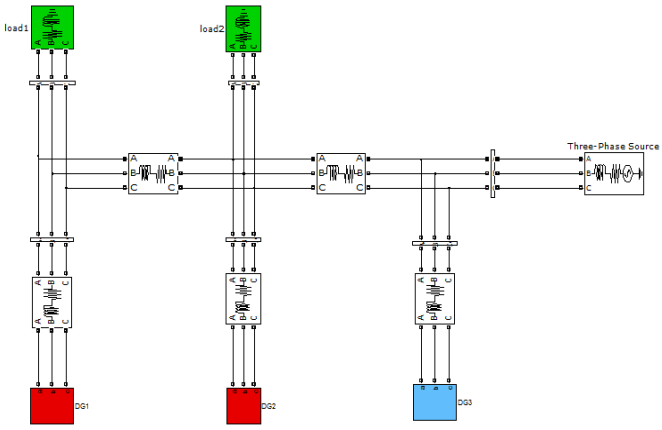

Figure 3: Simulink diagram of networked microgrid.

Table 1: DG System parameters [1]

Parameter		*Values*
Interfaced Inverter	Filter Inductor (L_f/R_f)	L:5mH/R:0.2Ω
	Filter Capacitor (C_f)	40μF
	Sampling-switching frequency	9kHz-4.5kHz
Microgrid parameters	Rated RMS voltage (Line-Line)	208V (60Hz)
	Total Loads	3525W-1425Var
Droop coefficients	Frequency droop D_p	0.00125 Rad / (Sec . W)
	Voltage droop D_Q	0.00143 V/Var
	Integral dead-band	6 W
	Integral gain K_c	0.0286 V/(Sec . W)
	LPF time constant τ	0.0159 Sec

The DG system parameters of the test system is detailed in Table 1.
The enhanced power control strategy is realized through the following two stages.

1) Stage 1: Initial Power Sharing Using Conventional Droop Method:
Before receiving the compensation flag signal, the conventional droop controllers are adopted for initial load power sharing. Meanwhile, the DG local controller monitors the status of the compensation flag dispatched from the microgrid central controller. During this stage, the steady-state averaged real power (P_{AVE}) shall also be measured for use in Stage 2. A moving average filter is used here to further filter out the power ripples. The measured average real power (P_{AVE}) is also preserved in this stage, so that when the synchronization signal flag changes, the last preserved value can be used for a reactive power sharing accuracy improvement control in Stage 2.

2) Stage 2: Power Sharing Improvement Through Synchronized Compensation:
In Stage 2, the reactive power sharing error is compensated by introducing a real-reactive power coupling transient and using an integral voltage magnitude control term. Once a compensation starting signal (sent from the central controller) is received by the DG unit local controller, the averaged real power calculation stops updating, and the last calculated P_{AVE} is preserved and used as an input for the compensation scheme. During the compensation process, the combination of both real and reactive powers is used in the frequency droop control, while the reactive power error is suppressed by using an additional integration term [15]. The reactive power compensation scheme is illustrated in Fig. 4.

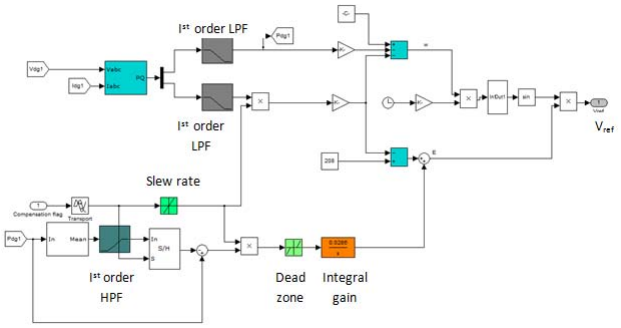

Figure 4: Reactive power compensation scheme at stage2.

The real power frequency control and reactive power voltage magnitude for the compensation is given by

$$\omega = \omega_0 - (D_P \cdot P + D_Q \cdot Q) \quad (8)$$

$$E = E_0 - D_Q \cdot Q + \left(\frac{K_C}{S}\right) \cdot (P - P_{AVE}) \quad (9)$$

Where K_C is the integral gain, which is selected to be the same for all the DG units.

It can be observed that with the control strategy in (8), the real and reactive power is coupled together for the frequency droop control. Compared to the conventional droop control, the reactive power droop term ($D_Q \cdot Q$) in (8) can be considered as an offset for the conventional real power droop control for frequency regulation. If there are any reactive power errors, the unequal offsets ($D_Q \cdot Q$) from different DG units will affect the DG output frequencies, which subsequently introduce the real power disturbances [16]. This real power disturbance will then cause the integral control term in (9) to regulate the DG output voltage. With this integral control, the real power from a DG will eventually be equal to P_{AVE}, meaning that accurate real power sharing is still maintained in Stage 2 (assume that there is no microgrid real power demand variations in the compensation period of Stage 2). Further consider that the modified frequency droop control in (9) essentially enables equal sharing of the combined power ($D_P \cdot P + D_Q \cdot Q$) in Stage 2; the accurate sharing of both the combined power and real power means that the reactive power sharing will also be accurate.

For instance, with the proposed control in (8), the DG units providing less reactive power in Stage 1 will experience a transient real power increase in Stage 2. Therefore, an integration of the real power difference ($P-P_{AVE}$) in a voltage magnitude control of (9) is able to eliminate the reactive power sharing error as discussed previously. Once the reactive power is shared properly, the DG unit real power flow will go back to its original value with the control of (8), and the integration control used in (9) will no longer contribute to the voltage magnitude regulation. Fig. 4, demonstrates the diagram of the proposed control strategy, where P_0 and Q_0 are the measured powers before LPF. When the compensation is not enabled, the conventional power sharing method as shown in (1) and (2) is adopted.

Once the compensation starts, the conventional control is replaced by (8) and (9). In Fig. 4, the unity soft compensation gain G is adopted for the proposed compensation method, which can avoid the excess power oscillations and current overshoots during the compensation transient. At the beginning of each compensation, the gain G will increase slowly to the rated value. After the compensation, G will decrease slowly to zero again, meaning that the droop controller is smoothly switched back to the conventional droop control mode.

The proposed method is developed based on the assumption that the real power load demand is constant during the compensation transient in Stage 2. For a real power load variation during the compensation stage, the proposed controller may leave some reactive power sharing errors after the compensation. There are two types of real power variations: steady-state real power variations/ ripples and microgrid load switching. To limit the impacts of small real power demand variations during the compensation transient, a dead band is placed before the integral control of the real power difference ($P-P_{AVE}$).

To avoid the impacts of large load demand variations or load switching in a microgrid, the compensation period should be properly designed by tuning the integral gain (K_C) in (9). A long compensation period will subject to possible microgrid load demand changes, while a too fast compensation will lead to excess transient and affect the accuracy as well. Considering that the variation of microgrid load demand, such as that in the residential area microgrids, is normally slow, a compensation time of a few seconds in Stage 2 is considered in this study.

A compensation dynamic of a few seconds also ensures that the compensation performance is not very sensitive to the "compensation flag" synchronization accuracy. Therefore, the requirements on the communication link bandwidth and the response time of DG unit local controllers can be quite low. For instance, even 0.1 sec inconsistency of starting the compensation will not cause any obvious performance differences as will be shown in the next section. Furthermore, if the compensation function is activated in every few minutes/hours, the proposed method can always maintain an accurate reactive power sharing without affecting the power quality. This is different from the method, where the non-characteristic harmonic current is injected into the system continuously.

Finally, note that the soft compensation gain and the dead band block are installed at the DG unit local controller. Also the compensation time (2 s in the simulations and experiments) is preset (by tuning the gain K_C) in the DG unit local controller and it is the same for all the DG units in the microgrid. Therefore, only the synchronized compensation start signals are required for the proposed controller. Any additional synchronized signals to terminate the compensation are unnecessary.

Flow control is critical need in many industrial processes. In this paper, we control the flow via two methods: PI and Fuzzy Logic Controller (FLC).

A. Simulation Results of PI Controller

For the system with PI controller shown in Fig. 4.7, proportional and integral gains are chosen as $K_p = 10$ & $K_i = 15.6$ and for the PI controller1 the proportional and integral gains are chosen as $K_p = 12$ & $K_i = 17.86$.

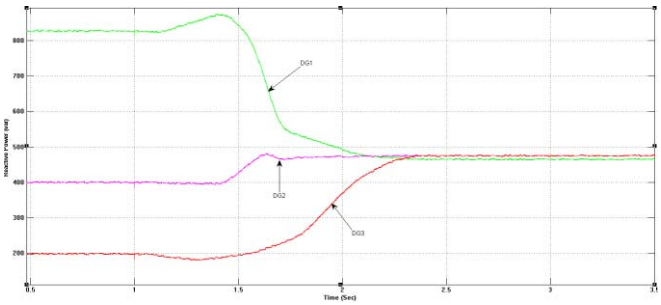

Figure 5: Reactive power sharing performance in a Network Microgrid using PI controller

Fig. 5 demonstrates the reactive power flow of the DG units. Due to unequal voltage drops on the networked microgrid feeders, the reactive power outputs of DG's is unequal and are treated as reactive power errors which can be observed in Fig. 5 which is also detailed in Table 2 with $t < 1$ sec. With the compensation brought in at $t = 1$ sec the reactive power sharing error is reduced almost to zero at $t = 2.3$ sec and the reactive power output of each DG is found to be 475 var.

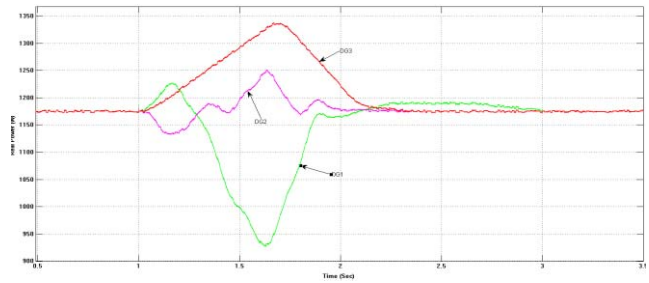

Figure 6: Real power sharing performance in a Network Microgrid using PI controller

Fig. 6 shows the real power output of the DG units. When the compensation is enabled at $t = 1.0$ sec, transient in the real power is seen ($1.0 \leq t < 3$) which is due to the transient real and reactive power coupling introduced by (10) and (11). However, the output real power settles down to the original value at around 3.0 sec as illustrated and detailed in Fig. 6 and Table 2 respectively.

Table 2: Real and Reactive powers of DG's before and after Compensation

DG Units	*Reactive Power (var)*		*Real Power (W)*	
	Before Compensation (t < 1 Sec)	*After Compensation (t > 3 Sec)*	*Before Compensation (t < 1 Sec)*	*After Compensation (t > 3 Sec)*
DG1	810	475	1175	1175
DG2	400	475	1175	1175
DG3	200	475	1175	1175

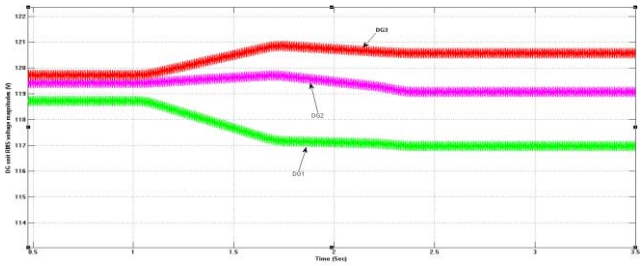

Figure 7: DG voltage magnitude using PI controller

Fig. 7 illustrates the changes of DG unit voltage magnitudes during the process of compensation. For equal reactive power sharing, these voltages have small deviations during the compensation. This is because the unequal voltage drops on the feeders are compensated by the DG units.

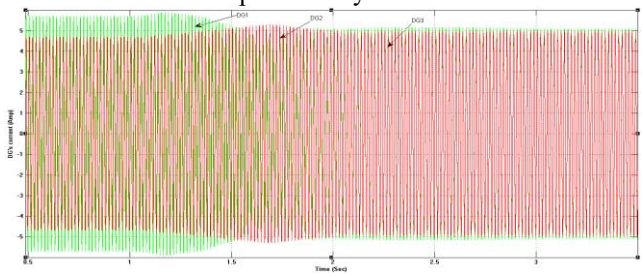

Figure 8: DG's current during compensation using PI controller

The DG line current waveforms before, during and after compensation is obtained as illustrated in Fig. 8 The current waveforms are also identical after the compensation. PI control is one of the earlier control strategies [1]. PI controller has a simple control structure which is easy to understand but the response of PI controller is not fast and reliable. To overcome this problem the PI controller is replaced with Fuzzy Controller so that the closed loop system exhibit small overshoot and settling time with zero steady state error.

B. Design of Fuzzy Logic Controller

Fig. 9 shows the simulink model of the Fuzzy Controller with unity feedback.

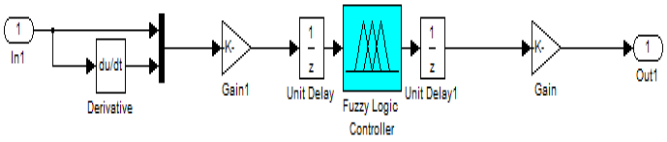

Figure 9: Simulink diagram of Fuzzy Controller

For the Fuzzy Interference System (FIS) considered in this work, Mamdani model with triangular membership function is chosen. The rule base used in the analysis is detailed in Table 3.

Table 3: Fuzzy Rule Base

Input error (e)	*Change in error (∫e)*							
	NB	**NM**	**NS**	**ZE**	**PS**	**PM**	**PB**
NB	NB	NB	NB	ZE	NM	NS	ZE
NM	NB	NB	NB	NM	NS	ZE	PS
NS	NB	NB	NM	NS	ZE	PS	PM
ZE	NB	NM	NS	ZE	PS	PM	PB
PS	NM	NS	ZE	PS	PM	PB	PB
PM	NS	ZE	PS	PM	PB	PB	PB
PB	ZE	PS	PM	PB	PB	PB	PB

Fig. 10 shows the reactive power output of DG units. The unequal reactive powers of DG's at $t < 1$ Sec which are reactive power errors are nullified with fuzzy controller. Both the PI and fuzzy controllers are in good agreement in making the reactive power errors to zero.

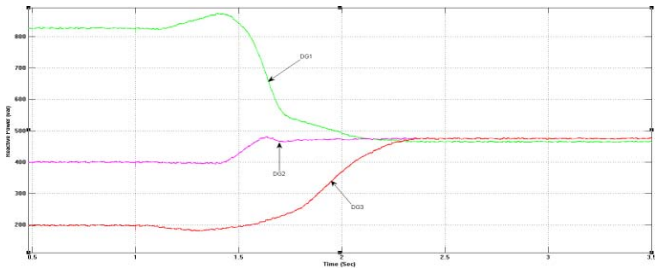

Figure 10: Reactive power sharing performance in a Network Microgrid using FLC

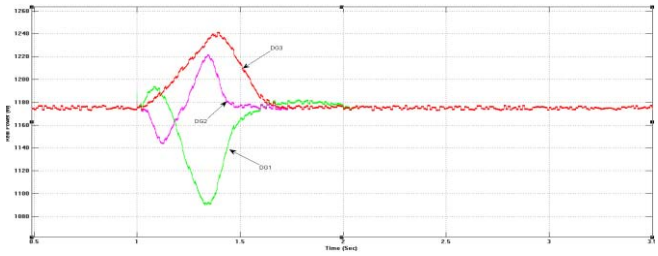

Figure 11: Real power sharing performance in a Network Microgrid using FLC.

Fig. 11 shows the real power output of DG units with FLC. Comparison of Fig. 11 with Fig. 6 reveals that the real power output settles down to original value at 2.1 sec as against 3 sec. Comparing Fig. 11 with Fig. 6, Table 4 is prepared depicting the performance of PI & FLC.

Table 4: Real Power Excursion during Compensation

DG Units	*Real Power peak (W)*		*Real Power settling time (Sec)*	
	PI	*Fuzzy*	*PI*	*Fuzzy*
DG1	930 @ 1.59 sec	1090 @ 1.38 sec	3	2.1
DG2	1250 @ 1.6 sec	1220 @ 1.32 sec	3	2.1
DG3	1340 @ 1.62 sec	1241 @ 1.4 sec	3	2.1

From Table 4, it can be concluded that the Fuzzy Logic Controller (FLC) is superior over PI controller.

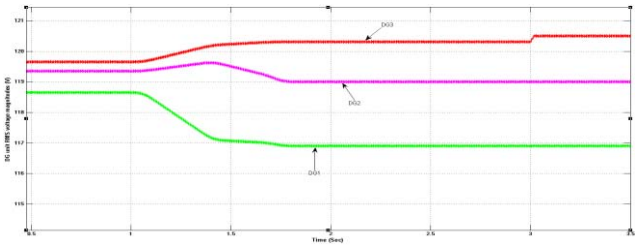

Figure 12: DG voltage magnitude using FLC

As per the objective of the work, i.e., equal reactive power sharing, the voltage magnitudes of the DG's changes during the process of compensation which is depicted in Fig. 12. Comparison of Fig. 12 with Fig. 7, reveals that the voltage of DG's is improved with Fuzzy Controller.

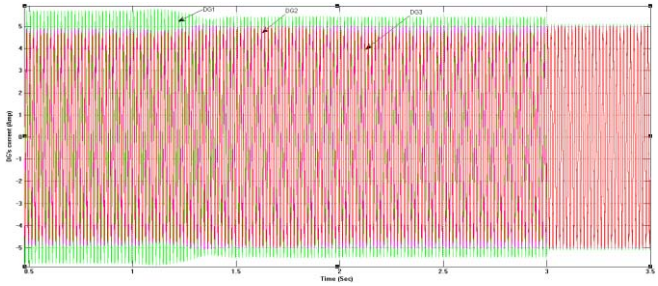

Figure 13: DG's current during compensation using FLC

By comparing Fig. 13 with Fig. 8, it can be concluded that the DG currents are reduced with Fuzzy Controller. From the results of both PI controller and fuzzy logic controller (FLC), the transients were reduced with FLC during compensation period and the errors were reduced after compensation. The time taken for attaining steady state is less in FLC compared to PI controller and the output is accurate in FLC.

4. Conclusion

This paper proposes an improved fuzzy logic based microgrid reactive power sharing strategy and results shows the vital role of fuzzy logic controller. In this method by injecting a real-reactive power transient coupling term for identifying the errors of reactive power sharing and then compensates the errors using a slow integral term for the DG voltage magnitude control. The compensation strategy also uses a low-bandwidth flag signal from the microgrid central controller to activate the compensation of all DG units in a synchronized manner. Therefore, accurate power sharing can be achieved while without any physical communications among DG units.

References

[1] J. Wei He and Y. W. Li, "An Enhanced Microgrid Load Demand Sharing Strategy," *IEEE Trans. Power Electron,* vol. 27, no. 27, pp. 3984-3995, Sep. 2012.

[2] J. He and Y. W. Li, "An accurate reactive power sharing control strategy for DG units in a microgrid," in *Proc. 8th Int. Conf. Power Electronics and ECCE Asia*, Jeju, Korea, pp. 551–556, 2011.

[3] Y. W. Li and C.-N. Kao, "An accurate power control strategy for power electronics-interfaced distributed generation units operation in a low voltage multibus microgrid," *IEEE Trans. Power Electron.*, vol. 24, no. 12,pp. 2977–2988, Dec. 2009.

[4] Kundur, P. ; Paserba, J. ; Ajjarapu, V. ; Andersson, G. "Definition and classification of power system stability," *IEEE Trans. Power systems*., vol. 19, no. 3, pp. 1387-1401, Aug. 2004.

[5] A. Mehrizi-Sani and R. Iravani, "Potential-function based control of a Microgrid in islanded and grid-connected modes," *IEEE Trans. Power Syst.,* vol. 25, no. 4, pp. 1883–1891, Nov. 2010.

[6] A. Tuladhar, H. Jin, T. Unger, and K.Mauch, "Control of parallel inverters in distributed AC power system with consideration of line impedance effect," *IEEE Trans. Ind. Appl.,* vol. 36, no. 1, pp. 131–138, Jan./Feb. 2000.

[7] E. A. A. Coelho, P. C. Cortizo, and P. F. D. Garcia, "Small-signal stability for parallel connected inverters in stand-alone AC supply systems," *IEEE Trans. Ind. Appl.*, vol. 38, no. 2, pp. 533–542, Mar./Apr. 2002.

[8] Y. Li and Y.W. Li, "Power management of inverter interfaced autonomous microgrid based on virtual frequency-voltage frame," *IEEE Trans. Smart Grid.,* vol. 2, no. 1, pp. 30–40, Mar. 2011.

[9] D M Tagare, *Reactive Power Management,* Tata McGraw Hill Publishers, 2004.

[10] D. N. Zmood and D. G. Holmes, "Stationary frame current regulation of PWM inverters with zero steady – state error," *IEEE Trans. Power Electron.,* vol. 18, no. 3, pp. 814-822, May 2003.

[11] J. M. Guerrero, L. G. Vicuna, J. Matas, M. Castilla, and J. Miret, "A wireless controller to enhance dynamic performance of parallel inverters in distributed generation systems," *IEEE Trans. Power Electron.,* vol. 19, no. 4, pp. 1205–1213, Sep. 2004.

[12] Y.W. Li, D. M. Vilathgamuwa, and P. C. Loh, "Design, analysis and real time testing of a controller for multi bus microgrid system," *IEEE Trans. Power Electron.*, vol. 19, no. 5, pp. 1195–1204, Sep. 2004.

[13] J. M. Guerrero, L. G. Vicuna, J. Matas, M. Castilla, and J. Miret, "Output impedance design of parallel-connected UPS inverters with wireless load sharing control," *IEEE Trans. Ind. Electron.,* vol. 52, no. 4, pp. 1126– 1135, Aug. 2005.

[14] N. Pogaku, M. Prodanovic, and T. C. Green, "Modeling, analysis and testing of autonomous operation of an inverter-based microgrid," *IEEE Trans. Power Electron.*, vol. 22, no. 2, pp. 613–625, Mar. 2007.

[15] K. D. Brabandere, B. Bolsens, J. V. D. Keybus, A.Woyte, J. Drisen, and R. Belmans, "A voltage and frequency droop control method for parallel inverters," *IEEE Trans. Power Electron.,* vol. 22, no. 4, pp. 1107–1115, Jul. 2007.

[16] Q. Zhang, "Robust droop controller for accurate proportional load sharing among inverters operated in parallel," *IEEE Trans. Ind. Electron.*, vol. 60, no. 4, Apr. 2013.